ELSEVIER

International Journal of Heat and Fluid Flow 21 (2000) 506–511

International Journal of HEAT AND FLUID FLOW

www.elsevier.com/locate/ijhff

On vortex generating jets

Zia U. Khan [a], James P. Johnston [b,*]

[a] A.T. Kearney, Inc., 153 East 53rd Street, New York, NY 10022, USA
[b] Department of Mechanical Engineering, Stanford University, Stanford, CA 94305-3030, USA

Abstract

Vortex generating jets (VGJs) are jets that pass through a wall and into a crossflow to create a dominant streamwise vortex that remains embedded in the boundary layer over the wall. The VGJ is characterized by its pitch and skew angles (Φ and Θ) and the velocity ratio (VR) between the jet and the crossflow. For VR = 1.0, the VGJ configuration of $\Phi = 30°$, $\Theta = 60°$ has been identified as that which produces the vortex with the highest peak mean vorticity. Three-component laser Doppler velocimetry (LDV) data for this particular configuration demonstrate many interesting features of the flow. Mean velocity data show a deficit of streamwise momentum in the core of the vortex, thinning of the boundary layer on the downwash side of the vortex, and thickening of the boundary layer on the upwash side. Plots of the turbulent kinetic energy and the turbulent shear stress $\langle uv \rangle$ show that the turbulent structure of the boundary layer is grossly disturbed by the presence of the vortex. The turbulent transport of the turbulent kinetic energy shows the possibility for a gradient diffusion model in most regions, but not the vortex core.

1. Introduction

Fig. 1 shows a diagram of the vortex generating jet (VGJ) and its defining parameters. The jet passes through a circular hole (the jet-hole) of diameter D in a wall over which the crossflow produces a turbulent boundary layer. The angle between the jet-hole centerline and the wall is the pitch angle, Φ. The angle between the projection of the centerline onto the wall and the crossflow (streamwise) direction is the skew angle, Θ. Because the jet is pitched with respect to the wall, the opening at the wall surface (the jet-orifice) is an ellipse. The skew angle can also be thought of as the angle between the major axis of the ellipse and the streamwise direction.

The origin of the coordinate system is located at the center of the jet-orifice. The streamwise direction is denoted by the x-coordinate; the direction normal to the wall by the y-coordinate; and the spanwise direction along the wall by the z-coordinate.

Although our study is of a single VGJ, spanwise rows of VGJs are particularly important in two engineering applications. The first application is boundary layer separation control, see Johnston (1999). Boundary layers separate when the streamwise momentum at the surface of the wall, and hence the wall shear stress, decreases to zero. The dominant streamwise vortex, which is embedded in the turbulent boundary layer, helps to prevent this by sweeping fluid with high streamwise momentum from the freestream towards the wall. Typically, in separation control applications, the spanwise spacing of the jet holes is equal to, or greater than $10D$, which is large enough that our study of a single VGJ may have direct application in the near field and even at 10–20 hole diameters downstream of injection.

The second application is film cooling, in which jets are used to provide a protective layer of cool fluid over a surface exposed to hot gases. Here, the sweeping of the hot freestream fluid towards the wall effected by the embedded vortex is not desirable. In film cooling applications, spanwise hole spacing is typically smaller than $5D$, and thus results described here at $x/D = 20$ may not be specifically applicable as spanwise mixing of adjacent vortex flows may have already occurred upstream near the jet-hole.

VGJs are qualitatively related to two canonical flows that have been studied in the past. The first flow is the normal jet in crossflow. Research in this flow has been extensively reviewed by Margason (1993) and recently discussed by Fric and Roshko (1994) and Kelso et al. (1996). Shi et al. (1991) discussed the vorticity dynamics in the near field of the normal jet that creates the symmetric counter-rotating vortex pair. Khan (1999) showed that these same vorticity dynamics gives rise to the dominant vortex of the VGJ. Andreopoulos and Rodi (1984) provided detailed turbulence measurements of the normal jet in crossflow.

The second flow, and one that is more relevant to the results being presented in this paper, is the embedded streamwise vortex in a turbulent boundary layer. Bradshaw (1987) reviewed turbulent flows with streamwise vorticity, including flows with vortices aligned in the streamwise direction. It was noted that most measurements show high values of turbulence in the core of the vortex. Since turbulence should be suppressed in the viscous core, these measurements are probably

* Corresponding author. Tel.: +1-650-723-4024; fax: +1-650-723-4548.

E-mail address: johnston@vonkarman.stanford.edu (J.P. Johnston).

0142-727X/00/$ - see front matter
PII: S0142-727X(00)00038-2

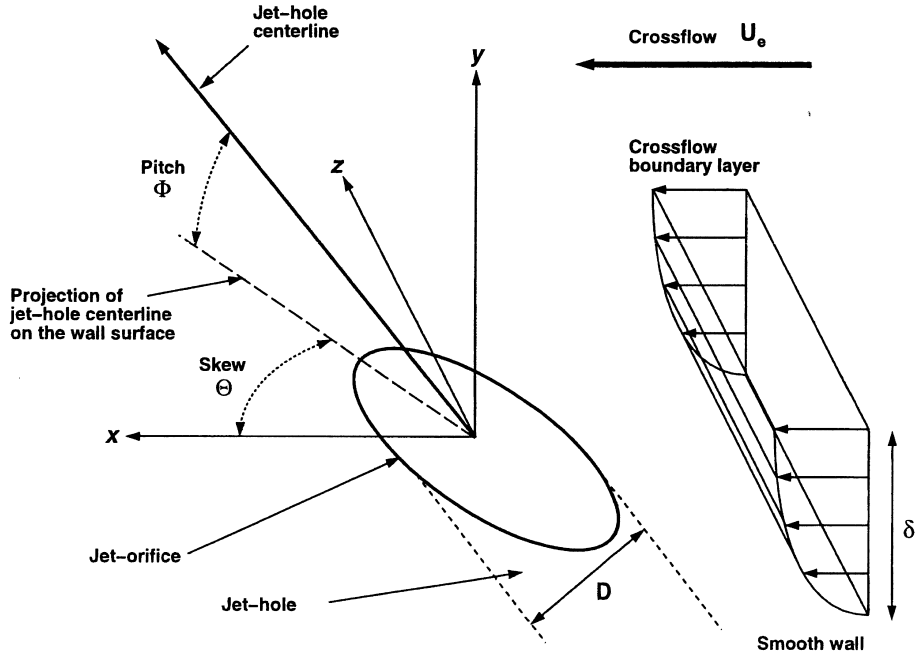

Fig. 1. VGJ defining parameters. The origin of the coordinate system is located at the center of the jet-orifice. Crossflow is right to left.

indicative of *vortex meandering*, or the wandering of the vortex in the measurement plane. We will return to this phenomena in the discussion of our own data. Shabaka et al. (1985), Pauley (1988), Westphal and Mehta (1989), and Cutler and Bradshaw (1993a,b) all performed experiments with either a single vortex or arrays of vortices embedded in turbulent boundary layers.

In addition to research in these two canonical flows, considerable work has been recently performed in VGJ flows themselves. Lin et al. (1990) reviewed various passive and active methods for controlling 2D turbulent separated flows. It was found that VGJs were highly effective compared to the more traditional solid vortex generators (generally tabs mounted on the surface) which have an additional drag penalty. Johnston and Nishi (1990) studied spanwise arrays of VGJs and demonstrated that they were effective in reducing the size of stalled regions of the flow. Compton and Johnston (1992) studied the flow from a single VGJ and confirmed that the vortex produced by the VGJ resembled that produced by solid vortex generators, but tended to decay somewhat faster downstream. Nishi et al. (1995) demonstrated that VGJs could enhance the pressure recovery in a diffuser. Honami et al. (1994) looked at VGJs for use in film cooling applications and found that the asymmetry of the flow reduced the film-cooling effectiveness of the jets. Zhang (1998) performed detailed LDV measurements that characterized the distributions of the turbulent stresses in the flow. Findlay et al. (1999) examined the effects of geometry (including spanwise hole spacing) and blowing ratio on jets from square holes. Finally, Johnston (1999) has reviewed a number of the foregoing papers, and many others, in connection with the use of VGJs in separation control.

2. Experiment

The research was performed using a low-speed free surface water channel. The jet was produced by a jet-hole in a wall plug, see Fig. 2. The plug could be rotated to vary the skew angle, and was mounted flush with surface of the test wall

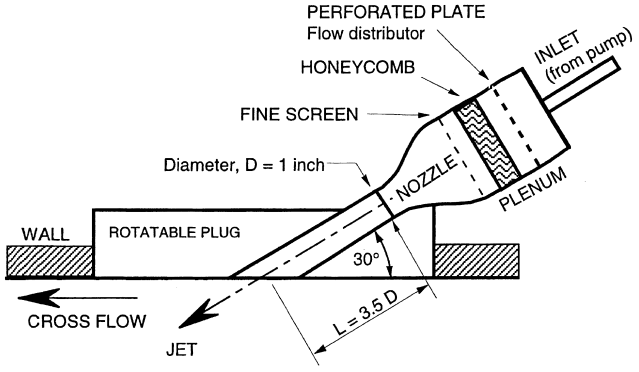

Fig. 2. Cross-section sketch of the jet-hole in the wall plug. Pitch angle fixed at 30°. Yaw angle varies by rotation of the plug about an axis perpendicular to the wall.

which was positioned vertically inside the water channel. The freestream velocity for the crossflow was $U_e = 0.2$ m/s. At the jet location, the boundary layer had a Reynolds number based on momentum thickness of 1100 and a thickness of 2 jet-hole diameters. The Reynolds number of the jet, based on jet-hole diameter ($D = 2.54$ cm) and mean jet speed, was 5000.

The short, cylindrical jet-hole was fed from a plenum through a smoothly rounded nozzle (area ratio, 4:1). Preliminary measurements taken at very high velocity ratios, where the crossflow has a minimal effect on the jet, indicate that the flow out of the jet was uniform except for the thin boundary layer that develops along the wall of the hole. The single jet-hole was located on the test wall at a spanwise (z) distance $10D$ below the free surface. Measurements up to $z = +9D$ showed no effect of the free surface boundary condition.

The measurements were made using a three-component laser Doppler velocimetry (LDV) system that composed of one two-component probe and one one-component probe. The probes were orthogonal to each other with intersecting

measuring volumes. Using the side scatter from the seed particles, each probe employed the other probe's receiving optics. This guaranteed that the measuring volumes from the two probes were coincident for all of the measurements. The measuring volume was spherical and approximately two viscous lengths in diameter.

Details of the experimental techniques can be found in Khan (1999).

3. Results and discussion

In our experiments, a number of VGJ configurations were studied at several downstream locations. The different VGJ configurations are shown in Table 1. In this paper, we will examine the results from just one configuration, the base case ($\Phi = 30°$, $\Theta = 60°$, and VR = 1.0) at one downstream location ($x/D = 20$). This geometrical configuration produced the strongest dominant vortex at VR = 1.0. Tabulated data for this configuration and the others listed in Table 1 are available Khan and Johnston (1999).

The distributions of the mean velocities, mean streamwise vorticity, turbulent kinetic energy, and $\langle uv \rangle$ shear stress distributions will be presented in this paper. Also, the mean velocity distribution at a plane just above the exit hole and parallel to the wall will be shown to demonstrate the exit conditions of the jet flow.

All quantities have been normalized by the freestream velocity, U_e, and the jet-hole diameter, D.

3.1. Mean velocities and streamwise vorticity

The mean velocity distribution at the jet exit is shown in Figs. 3 and 4. The horizontal axis is the streamwise direction (x/D), and the vertical axis is the spanwise direction (y/D). The contours represent the velocity out of the page in the wall-normal direction, V. The vectors represent the velocities in the plane parallel to the wall, (U, W). Several interesting features come to light. The crossflow sweeps around the $-z$ side of the orifice much like the potential flow around an elliptical object. However, at the $+z$ side of the orifice, the jet flow deflects the near-wall crossflow rather abruptly. Also, it can be seen from the velocity contours that the jet does *not* exit the jet-hole uniformly at this low velocity ratio as it did at high VR values. A narrow region of high V velocity component with a steep shear layer are seen on the downstream side of the inclined jet, distortions with their origins inside the jet-hole as shown in flow visualization by Khan (1999).

The mean velocity distribution at the downstream location, $x/D = 20$, is shown in Fig. 5. The horizontal axis is the spanwise direction (z/D), and the vertical axis is the wall-normal (y/D). Note that this is the configuration for the rest of the plots discussed in the paper. The contours represent the streamwise velocity U. The streamwise ($+x$) direction in this and subsequent plots is into the page, away from the reader. The vectors represent the secondary flow (V, W). A reference vector with velocity magnitude $0.2U_e$ is shown at the top of the plot.

Table 1
Parameter variation cases

Case names	VR	Θ (°)	Φ (°)
Base	1.0	60	30
$\Theta = 45°$	1.0	45	30
$\Theta = 90°$	1.0	90	30
$\Phi = 45°$	1.0	60	45
VR = 1.5	1.5	60	30

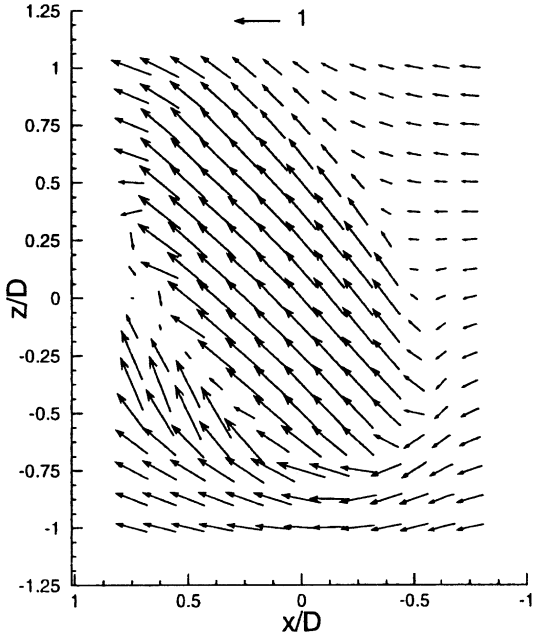

Fig. 3. Mean velocities at the jet-orifice. Plane of data is parallel to the wall, located at $y/D = 0.1$. The vectors indicate velocity in the plane with components (U, W). Reference vector for flow velocity magnitude equal to $1.0U_e$ is shown at the top.

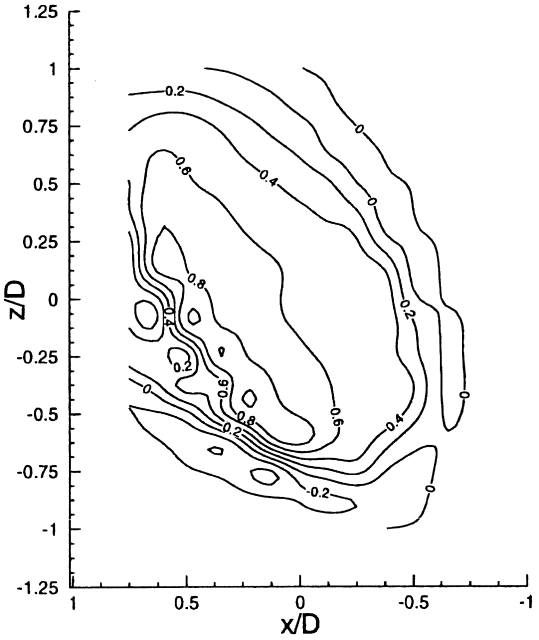

Fig. 4. Mean velocity contours of V at the jet-orifice plane. Plane of data is the same as in previous figure.

The thinning of the boundary layer on the downwash side of the vortex and the thickening of the boundary layer on the upwash side are both clear from the streamwise velocity contours. The secondary flow is quite strong near the wall, reaching velocity magnitudes of up to $0.2U_e$. There is a streamwise velocity deficit in the vortex core, where U is only

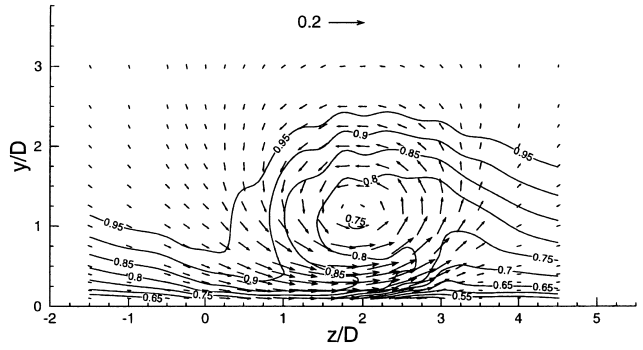

Fig. 5. Distribution of mean velocities. Contours are for streamwise velocity U; vectors are for secondary flow (V, W). Reference vector is shown at top plot for vector of magnitude $0.2U_e$.

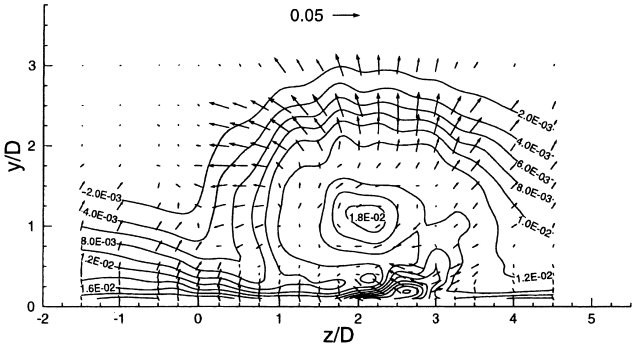

Fig. 7. Distribution of q^2 (contours) and turbulent transport of q^2 (vectors). Reference vector at top.

0.75. This is believed to be the result of movement of low speed boundary layer fluid up into the core region by the strong secondary flow upstream of this location. However, "vortex bursting" in the regions of vortex formation, very close to the jet-hole may also play a role.

The secondary flow streamlines are somewhat oval-shaped in the core region. This may result from vortex meandering in the spanwise direction, or it may result simply from the "flattening" effect of the wall which may be represented by a potential flow model with an image vortex to represent the wall. Flow visualization at these experimental conditions revealed that the vortex incurs random spanwise movements. This suggests that vortex meander is the more likely cause of oval-shaped secondary streamlines.

The mean streamwise vorticity distribution, obtained from gradients of V and W, is shown in Fig. 6. There are two distinct vortical regions: the negative region associated with the vortex and the positive region associated with the spanwise shear layer created by the secondary flow over the wall. The negative vorticity contours appear to be twin-lobed. This shape is the result of the oval-shaped secondary flow streamlines around the core of the vortex. The positive vorticity is located primarily in the near-wall upwash region.

Extensive studies of the mean flow by visualization using various dye techniques support the conclusions reached from this brief discussion of the quantitative data, see Khan (1999) for details.

3.2. Turbulence quantities

The turbulent kinetic energy, $q^2/2$, is shown in Fig. 7 (as contours of q^2). The turbulence levels in the near-wall upwash region are quite high because the secondary flow is convecting highly turbulent flow from very close to the wall upwards. The turbulence levels in the core are also quite high. The most likely reason for this is vortex meandering, in which the moving vortex creates artificial turbulence through the Reynolds averaging of an unsteady flow.

The turbulent transport of q^2 can be characterized by the transport vectors (V_q, W_q) defined as:

$$V_q = \frac{\langle q^2 v \rangle}{q^2}, \quad W_q = \frac{\langle q^2 w \rangle}{q^2}.$$

Fig. 7 shows the vectors of the turbulent transport superimposed over the contours of q^2. For most regions, the vectors are perpendicular to the contours and their magnitude is correlated to the relative proximity of adjacent contours. Both these phenomena imply that in these regions gradient modeling of the turbulent transport of q^2 may be appropriate.

However, in the core of the vortex this is no longer the case. Here, it is clear that the vectors are not perpendicular to the contours. In fact it appears that the vectors are tangential to the contours and are oriented in a direction opposite that of the secondary flow. This strange behavior can also be seen in the data of Pauley (1988).

The production of turbulent kinetic energy can be determined if the slender flow approximation (that gradients in the x-direction are negligible) is used. The distribution of q^2 production is shown in Fig. 8. The production is strongest near the wall and in the upwash region close to the wall. Elsewhere the turbulence energy is small. It is decaying in the core region and away from the wall.

Although the three-component LDV system allows us to measure all three shear stresses, in this paper only the most important component, $\langle uv \rangle$, will be discussed.

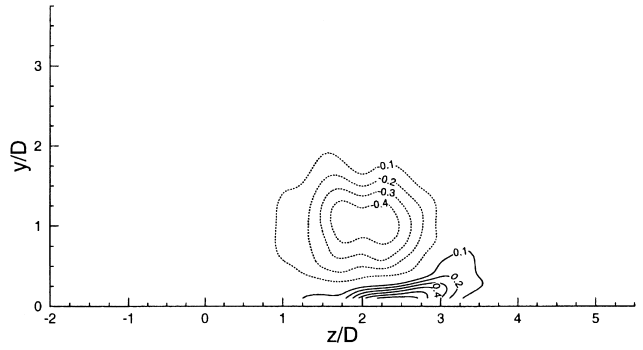

Fig. 6. Distribution of mean streamwise vorticity. Dashed lines indicate negative values.

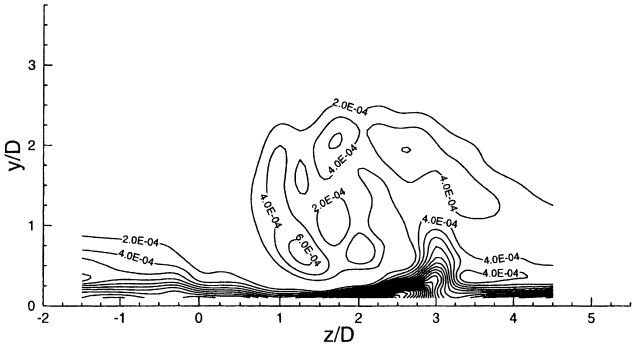

Fig. 8. Distribution of turbulent kinetic energy production.

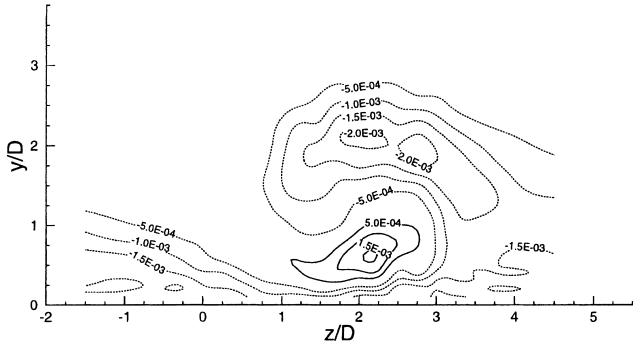

Fig. 9. Distribution of $\langle uv \rangle$.

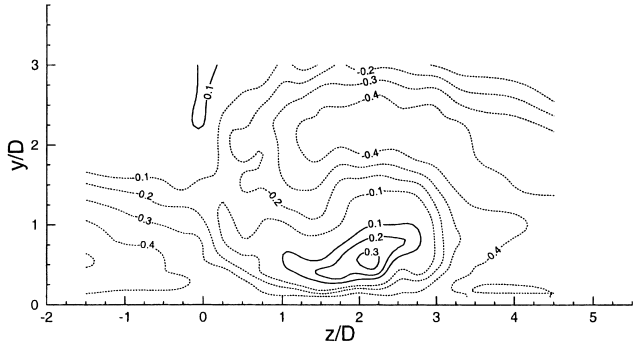

Fig. 10. Distribution of R_{uv}.

Fig. 9 shows the distribution of $\langle uv \rangle$. There are three principal regions: negative $\langle uv \rangle$ at the top of the vortex core, positive $\langle uv \rangle$ below the vortex core, and negative $\langle uv \rangle$ in the thinned and thickened portions of the boundary layer. The positive values for $\langle uv \rangle$, which is normally negative in wall-bounded shear flows, arise from the fact that U decreases with increasing y in the region below the vortex. The negative values for $\langle uv \rangle$ on top of the vortex arise from the fact that U increases from the low speed vortex core region to the freestream with increasing y.

The correlation coefficient for $\langle uv \rangle$, R_{uv}, is shown in Fig. 10. It can be seen that the negative region of $\langle uv \rangle$ on top of the vortex, and to a lesser degree the other two regions, are highly correlated. This means that the $\langle uv \rangle$ distributions reflect correlated stresses and are not simply the result of augmented values of $\langle uu \rangle$ or $\langle vv \rangle$ due the presence of the embedded vortex in the boundary layer.

4. Conclusions

The principal conclusions of this paper are:

- The jet flow did not exit the jet-orifice uniformly. The near field flow close to, and inside, the jet-hole was substantially disturbed by the interaction of the jet and the crossflow.
- The VGJ produced a dominant vortex that remained embedded in the boundary layer. At high VR values or for very thin boundary layers ($\delta \ll D$), the vortex may penetrate the boundary layer, but such was not the case here.
- The secondary flow associated with the vortex has the effect of thinning the boundary layer on the downwash side and thickening it on the upwash side.
- The core of the vortex has a streamwise momentum deficit.
- The vortex enhances the turbulence levels in the boundary layer, particularly near the wall, under the vortex core where production is large.
- The turbulent transport of turbulent kinetic energy may be represented by a turbulent diffusion model, except in the vortex core region.
- The shear stress $\langle uv \rangle$ distribution of the boundary layer is distorted by the vortex, with a region of positive $\langle uv \rangle$ being created in the mean shear layer between the vortex core and the wall. These stresses are well correlated and are not simply the result of augmented levels of $\langle uu \rangle$ and $\langle uv \rangle$.

Acknowledgements

The research was supported by the National Science Foundation and the Affiliates of the Thermal and Fluid Sciences. We are also in debt to many individuals, in particular to Professors John Eaton and Peter Bradshaw.

References

Andreopoulos, J., Rodi, W., 1984. Experimental investigation of jets in crossflow. Journal of Fluid Mechanics 138, 93–127.

Bradshaw, P., 1987. Turbulent secondary flow. Annual Review of Fluid Mechanics 19, 53–74.

Compton, D.A., Johnston, J.P., 1992. Streamwise vortex production by pitched and skewed jets in a turbulent boundary layer. AIAA Journal 30, 640–647.

Cutler, A.D., Bradshaw, P., 1993a. Strong vortex/boundary layer interactions. Part I. Vortices high. Experiments in Fluids 14, 321–332.

Cutler, A.D., Bradshaw, P., 1993b. Strong vortex/boundary layer interactions. Part II. Vortices low. Experiments in Fluids 14, 393–401.

Findlay, M.J., Salcudean, M., Gartshore, I.S., 1999. Jets in crossflow: effects of geometry and blowing ratio. ASME Journal of Fluids Engineering 121, 373–378.

Fric, T.F., Roshko, A., 1994. Vortical structure in the wake of a transverse jet. Journal of Fluid Mechanics 279, 1–47.

Honami, S., Shizawa, T., Uchiyama, A., 1994. Behavior of the laterally injected jet in film cooling: measurements of surface temperature and velocity/temperature field within the jet. ASME Journal of Turbomachinery 116, 106–112.

Johnston, J.P., Nishi, M., 1990. Vortex generator jets – means for flow separation control. AIAA Journal 28, 429–436.

Johnston, J.P., 1999. Pitched and skewed vortex generator jets for control of turbulent boundary layer separation: a review. In: Paper FEDSM99-6917, Proceedings of the Third ASME/JSME Joint fluids Engineering Conference, 16–23 July. San Francisco, CA, USA.

Kelso, R.M., Lim, T.T., Perry, A.E., 1996. An experimental study of round jets in cross-flow. Journal of Fluid Mechanics 306, 111–144.

Khan, Z.U., Johnston, J.P., 1999. On the dominant vortex produced by a pitched and skewed jet in crossflow, volume 2. Report No. TSD-123, Thermosciences Division, Mechanical Engineering Department, Stanford University, Stanford, CA 94305-3030.

Khan, Z.U., 1999. On the dominant vortex produced by a pitched and skewed jet in crossflow. Ph.D. thesis, Stanford University, Stanford, CA; Also, Report No. TSD-122, Thermosciences Division, Mechanical Engineering Department, Stanford University, Stanford, CA 94305-3030.

Lin, J.C., Howard, F.G., Bushnell, D.M., 1990. Investigation of several passive and active methods for turbulent flow separation control. AIAA 90-1598.

Margason, R.J., 1993. Fifty years of jet in cross flow research. In: Computational and Experimental Assessment of Jets in Cross Flow, AGARD-CP-534.

Nishi, M., Shibata, Y., Nadamura, M., Okamoto, 1995. Application of vortex generator jets to control the flow from separating in a

conical diffuser. In: Separated and Complex Flows, ASME FED – Vol 217, pp. 27–34.

Pauley, W.R., 1988. The fluid dynamics and heat transfer effects of streamwise vortices embedded in a turbulent boundary layer. Ph.D. thesis, Stanford University, Stanford, CA.

Shabaka, I.M.M.A., Mehta, R.D., Bradshaw, P., 1985. Longitudinal vortices embedded in turbulent boundary layers. Part 1. Single vortex. Journal of Fluid Mechanics 155, 37–57.

Shi, Z., Wu, J.Z., Wu, J.M., 1991. Symmetric and asymmetric jets in a uniform crossflow. AIAA 91-0722.

Westphal, R.V., Mehta, R.D., 1989. Interaction of an oscillating vortex with a turbulent boundary layer. Experiments in Fluids 7, 405–411.

Zhang, X., 1998. Turbulence measurements of a longitudinal vortex generated by an inclined jet in a turbulent boundary layer. ASME Journal of Fluids Engineering 120, 1–7.